Int. J. Heat Mass Transfer. Vol. 9, pp. 773–789. Pergamon Press 1966. Printed in Great Britain

HEAT TRANSFER TO MHD FLOW IN THE THERMAL ENTRANCE REGION OF A FLAT DUCT*

CHING-LAI HWANG†, P. J. KNIEPER‡ and LIANG-TSENG FAN§
Kansas State University, Manhattan, Kansas

(*Received* 12 *July* 1965 *and in revised form* 13 *January* 1966)

Abstract—Heat transfer to an MHD fluid in the thermal entrance region of a flat duct has been investigated. The flow is laminar and fully developed Hartmann flow, and heat flux at the wall is considered to be constant. The developing temperature profiles as well as the local Nusselt number are presented graphically for the heat generation parameter of −1·0, −0·5, 0, 0·5 and 1·0; for the Hartmann number of 0, 4 and 10; and for the electric field factor of 0·5, 0·8 and 1·0. The results presented are applicable for the cases with any Prandtl number. Comparisons are presented for certain cases with the previous work.

NOMENCLATURE

A, surface area of channel walls through which heat is being transferred;
a, one-half of duct height;
A_k, B_k, C_k, D_k, constants defined by equation (11);
B_0, magnetic field induction;
C_p, specific heat;
D_e, equivalent diameter of the duct, $4a$;
E, electric field strength;
e, $= \dfrac{E}{u_0 B_0}$, electric field magnitude factor;
H, magnetic field intensity;
H_0, magnetic field imposed perpendicular to bounding walls;
h, heat-transfer coefficient;
J, electric current density;
k, thermal conductivity;
M, $= \mu_e H_0 a\sqrt{(\sigma_e/\mu)}$, Hartmann number;
Nu_x, $= \dfrac{h_x D_e}{k}$, local Nusselt number;
p, fluid pressure gradient in equation (1);
Pr, $= \dfrac{\mu C_p}{k}$, Prandtl number;
q_x, rate of heat transfer;
q'', $= \dfrac{-q}{A}$, negative rate of heat transfer per unit area;
Re_a, $= \dfrac{\rho u_0 a}{\mu}$, Reynolds number;
t, temperature;
t_0, temperature of fluid at entrance of channel;
U, $= \dfrac{u}{u_0}$, dimensionless velocity;
u, velocity in x-direction;
u_0, average fluid velocity;
V, fluid velocity vector;
X, $= \dfrac{kx}{\rho a^2 u_0 C_p} = \dfrac{x/a}{Re_a Pr}$, dimensionless variable distance along length of duct;
x, variable distance along length of duct;
Y, $= y/a$, dimensionless variable distance across height of duct;
y, variable distance across height of duct;
z, variable distance along width of duct.

Greek symbols

η, $= \dfrac{u_0^2 \mu}{a q''}$, heat-generation parameter;

* This study was supported by the Air Force Office of Scientific Research Grant AF-AFOSR-463-64 and AF-AFOSR-463-66.
† Assistant Professor of Mechanical Engineering.
‡ Graduate Research Assistant in Chemical Engineering.
§ Professor of Chemical Engineering.

ρ, density;
μ, viscosity;
μ_e, magnetic permeability;
σ_e, electric conductivity;
τ, time;
θ, $= \dfrac{t - t_0}{aq''/k}$, dimensionless temperature;
ψ, $= \dfrac{-4}{\Delta\theta}$, pseudo-local Nusselt number.

Subscripts
b, bulk property or mean fluid property;
j, at jth position along x-axis;
k, at kth position along y-axis;
w, at walls or plates;
x, local property at position x.

INTRODUCTION

THE study of heat transfer in an electrically conducting fluid flowing within a magnetic field has become quite important. This is due to the development of such devices as magnetohydrodynamic accelerators, generators, and similar devices. A flat duct considered in this work has applications in such devices.

The general literature on MHD heat transfer before 1962 is well summarized by Romig [1]. Siegel [2] investigated heat transfer to the region where the temperature distribution is fully developed and the heat flux at the wall is uniform. Alpher [3], Yen [4], and Snyder [5] investigated the same problem but they assumed that the duct walls are electrically conducting. Regirer [6] and Gershuni and Zkukhovitskii [7] studied the problem but neglected the Joule heating in the fluid.

The case considering constant wall temperature with viscous and electrical dissipation in the thermal entrance region was investigated by Nigam and Singh [8]. However, the Joule heating term in this investigation was incorrectly represented [9], rendering their results invalid. Erickson *et al.* [10] using a finite difference analysis, presented the results for this case. Jain and Srinivasan [11] extended this problem to include the effects of electrically conducting walls.

Michiyoshi and Matsumoto [12] studied both the case of constant wall temperature and the case of uniform heat flux at the wall, but neglected the heat produced by viscous dissipation. They considered only the open circuit case, that corresponds to $e = 1{\cdot}0$.

The problem investigated in this work is the heat transfer to an MHD fluid for the case of uniform heat flux at the wall in the thermal entrance region. Neither viscous dissipation nor Joule heating is neglected, and there can be a net electric current flow parallel to the wall and perpendicular to the flow direction. This same problem was investigated previously by Perlmutter and Siegel [9]. They separated the problem into two parts: a problem which has a specified uniform heat flux at the wall but no internal heat generation in the fluid, and a problem which has internal heat generation within the fluid but no heat transfer at the channel wall. By the superposition of these two separate solutions, one can obtain the general solution and the temperature distribution. The solution for each part of the problem is presented in graphical form for certain cases. It is, however, rather tedious and difficult to carry out the superposition and obtain a temperature distribution at any position for any desired case. Also the overall effects of various parameters on the heat transfer are not obvious in this type of presentation.

The purpose of this paper is to present the results of the problem in an easily interpretable manner so that the overall effects of the various parameters can easily be demonstrated.

The developing temperature profiles and the local Nusselt number for the heat-generation parameter of $-1{\cdot}0$, $-0{\cdot}5$, 0, $0{\cdot}5$ and $1{\cdot}0$ are presented for the Hartmann number of 0, 4 and 10. The results are compared with those obtained by other investigators.

BASIC EQUATIONS

The geometry under consideration, illustrated in Fig. 1, consists of two semi-infinite parallel plates extending in the x- and z-directions. The electrically conducting fluid flows in the x-direction, the magnetic field is imposed in the y-direction, and the electric current flows in the z-direction. We consider the steady, laminar,

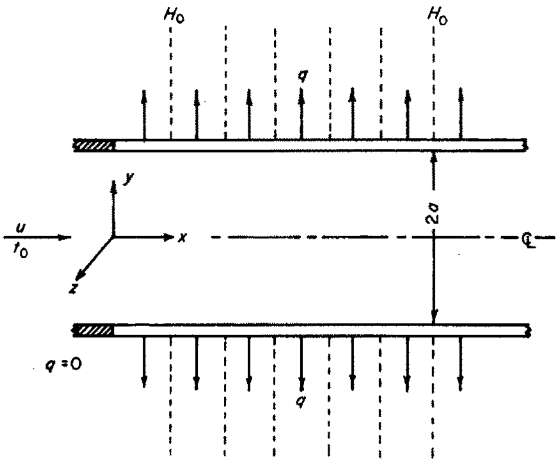

FIG. 1. Parallel plate channel with imposed uniform wall heat flux and transverse magnetic field.

incompressible, and fully developed Hartmann flow, and the physical properties of fluid are independent of temperature and are constant.

The fully developed velocity profile was originally obtained by Hartmann [13]. Cowling [14] gave the Hartmann velocity profile for zero net current in the following form:

$$u = \frac{pM}{\sigma_e \mu_e^2 H_0^2}\left[\frac{\cosh M - \cosh M(y/a)}{\sinh M}\right] \quad (1)$$

where p is fluid pressure gradient; M is Hartmann number, equivalent to $\mu_e H_0 a\sqrt{(\sigma_e/\mu)}$; μ_e is magnetic permeability, σ_e is electric conductivity, and H_0 is applied magnetic field. The average value of μ between $y = \pm a$ is

$$u_0 = \frac{\int_{-a}^{a} u \, dy}{\int_{-a}^{a} dy} = \frac{p}{\sigma_e \mu_e^2 H_0^2}[M \cosh M - 1]. \quad (2)$$

Then the dimensionless velocity profile used in this work is

$$\frac{u}{u_0} = U = M\left[\frac{\cosh M - \cosh M(y/a)}{M \cosh M - \sinh M}\right], \quad (3)$$

which is independent of the electric field.

The general form of the energy equation for unidirectional steady flow of an incompressible fluid with constant properties and with negligible heat conduction in the fluid flow direction can be simplified to

$$u\frac{\partial t}{\partial x} = \frac{k}{\rho C_p}\frac{\partial^2 t}{\partial y^2} + \frac{\mu}{\rho C_p}\left(\frac{\partial u}{\partial y}\right)^2 + \frac{J^2}{\rho C_p \sigma_e}. \quad (4)$$

The electric current intensity J can be expressed by

$$J = u_0 \sigma_e B_0 \left[-e + \frac{u}{u_0}\right] \quad (5)$$

where e is the electric field magnitude factor.

With this value for J, the energy equation becomes

$$u\frac{\partial t}{\partial x} = \frac{k}{\rho C_p}\frac{\partial^2 t}{\partial y^2} + \frac{\mu}{\rho C_p}\left(\frac{\partial u}{\partial y}\right)^2 + \frac{u_0^2 \sigma_e B_0^2}{\rho C_p}\left(-e + \frac{u}{u_0}\right)^2. \quad (6)$$

Introducing the dimensionless parameters

$Pr = \frac{\mu C_p}{k}$, Prandtl number,

$U = \frac{u}{u_0} = M\left[\frac{\cosh M - \cosh MY}{M \cosh M - \sinh M}\right]$,

$X = \frac{kx}{\rho a^2 \mu_0 C_p} = \frac{x/a}{Re_a Pr}$,

$Y = \frac{y}{a}$,

$\theta = \frac{t - t_0}{q''a/k}$,

$\eta = \frac{u_0^2 \mu}{q''a}$, heat-generation parameter,

equation (6) then becomes

$$U\frac{\partial \theta}{\partial X} = \frac{\partial^2 \theta}{\partial Y^2} + \eta\left(\frac{\partial U}{\partial Y}\right)^2 + M^2 \eta (e - U)^2. \quad (7)$$

The boundary conditions are

$$
\begin{aligned}
&1.\quad \theta = 0 \quad \text{at} \quad X = 0 \quad \text{and} \quad 0 \leqslant Y \leqslant 1,\\
&2.\quad \frac{\partial\theta}{\partial X} = 0 \quad \text{at} \quad Y = 0 \quad \text{and} \quad 0 < X,\\
&3.\quad \frac{\partial\theta}{\partial Y} = 1 \quad \text{at} \quad Y = 1 \quad \text{and} \quad 0 < X.
\end{aligned} \tag{8}
$$

The third boundary condition can be developed from the assumption of constant heat flux at the wall [15].

SOLUTIONS OF THE ENERGY EQUATIONS

In order to solve the energy equation, the velocity profile is first determined from equation (3) and the energy equation is solved by employing a finite difference analysis. The finite difference equations are (see Fig. 2 for the mesh network)

$$
\begin{aligned}
U &= U_{j,k},\\
\frac{\partial\theta}{\partial Y} &= \frac{\theta_{j,k+1} - \theta_{j,k-1}}{2\Delta Y},\\
\frac{\partial\theta}{\partial X} &= \frac{\theta_{j+1,k} - \theta_{j,k}}{\Delta X},\\
\frac{\partial^2\theta}{\partial Y^2} &= \frac{(\theta_{j+1,k+1} - 2\theta_{j+1,k} + \theta_{j+1,k-1})}{2(\Delta Y)^2} + \frac{(\theta_{j,k+1} - 2\theta_{j,k} + \theta_{j,k-1})}{2(\Delta Y)^2},\\
\frac{\partial U}{\partial Y} &= \frac{(U_{j+1,k+1} - U_{j+1,k-1})}{2\Delta Y}.
\end{aligned} \tag{9}
$$

The boundary conditions in the finite difference form become

$$
\begin{aligned}
&1.\quad \theta_{0,k} = 0 \quad \text{at} \quad X = 0 \quad \text{and} \quad 0 \leqslant Y \leqslant 1,\\
&2.\quad \theta_{j+1,2} = \theta_{j+1,0} \quad \text{at} \quad X > 0 \quad \text{and} \quad Y = 0,\\
&3.\quad \theta_{j+1,n+1} = \theta_{j+1,n} + \Delta Y \quad \text{at} \quad X > 0 \quad \text{and} \quad Y = 1.
\end{aligned} \tag{10}
$$

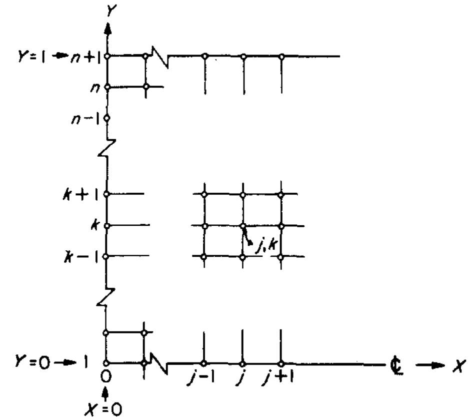

FIG. 2. Mesh network for difference representations.

Substituting the difference equations, equation (9), into the energy equation, equation (7), the following equation, in which the θ terms with subscript $j + 1$ are the unknowns and the θ terms with subscript j are the known variables, is obtained.

$$
[C_k]\theta_{j+1,k+1} + [A_k]\theta_{j+1,k} + [B_k]\theta_{j+1,k-1} = [D_k], \tag{11}
$$

where

$$
\begin{aligned}
[C_k] &= [B_k] = -\frac{1}{2(\Delta Y)^2},\\
[A_k] &= \frac{U_{j,k}}{\Delta X} + \frac{1}{(\Delta Y)^2},\\
[D_k] &= -[C_k]\,\theta_{j,k+1} - \frac{1}{(\Delta Y)^2}\theta_{j,k} - [C_k]\,\theta_{j,k-1} + \frac{U_{j,k}}{\Delta X}\theta_{j,k} + \frac{\eta}{4(\Delta Y)^2}\\
&\quad \times (U_{j+1,k+1} - U_{j+1,k-1})^2 + M^2\eta(e - U_{j,k})^2.
\end{aligned}
$$

Substituting $k = 1, 2, \ldots, n$ into equation (11) with the boundary conditions given by equation (10), n unknowns and n simultaneous equations are obtained. These equations are solved by the Thomas method [16]. It is important to achieve convergence to the true solution of the differential equations within the available computer storage capacity. When the value of $\frac{U(\Delta Y)^2}{12(\Delta X)}$ is kept less than 0·05, the truncation errors are reduced from $0(\Delta X)$ and $0(\Delta Y^2)$ to $0(\Delta X^2)$ and $0(\Delta Y^4)$ [10, 17]. Although the velocity, U, is in the range, $0 \leqslant U \leqslant 1{\cdot}5$, it is taken as 1·0 in calculating the values of $\frac{U(\Delta Y)^2}{12(\Delta X)}$. The mesh sizes employed are shown in Table 1.

Table 1. Mesh sizes for finite difference solution of the energy equation

X	ΔX	ΔY	N	$\frac{U(\Delta Y)^2}{12(\Delta X)}$
0–0·001	0·0005	0·00625	160	0·0065
0·001–0·01	0·001	0·0125	80	0·013
0·01–0·1	0·005	0·0125	80	0·0026
0·1–2·5	0·01	0·0125	80	0·0013

HEAT TRANSFER PARAMETERS

The bulk temperature (or mixing mean temperature) is evaluated after the temperature profile has been determined by the following finite difference equation at $X = (j + 1)\Delta X$

$$\theta_{b,X} = \sum_{k=1}^{n} \theta_{j+1,k} U_{j+1,k} \Delta Y. \tag{12}$$

The wall temperature is approximated in finite difference form as [15]

$$\theta_{w,X} = \theta_{j+1,n+1} = \frac{4\theta_{j+1,n} - \theta_{j+1,n-1} + 2\Delta Y}{3}. \tag{13}$$

The mean Nusselt number, Nu_m, for constant heat flux at the wall is of secondary importance, and the local Nusselt number, Nu_x, is desired. The local Nusselt number may be used to evaluate the wall temperature at any position along the duct whereas the primary usefulness of the mean Nusselt number is in evaluating the temperature of fluid leaving the heat exchanger. The local Nusselt number is defined as

$$Nu_x = \frac{h_x D_e}{k}. \tag{14}$$

For the case of constant heat flux at the wall, the local Nusselt number reduces to [15, 17]

$$Nu_X = \frac{-4}{\Delta\theta} \tag{15}$$

where $\Delta\theta$ is the difference of the wall temperature and the bulk temperature defined as

$$(\Delta\theta)_X = \theta_{w,X} - \theta_{b,X}.$$

RESULTS AND DISCUSSION

The results for the following parameters are presented: the Hartmann number of 0, 4 and 10; the electric field factor of 0·5, 0·8 and 1·0; and the heat-generation parameter of −1·0, −0·5, 0, 0·5 and 1·0. The results presented are applicable to any Prandtl number.

The electric field factor, e, is equivalent to the efficiency of an MHD generator and may be defined as the ratio of the electric power developed to the power necessary to produce the flow of the fluid. The value of e for the maximum power generation is 0·5. The generally accepted value of e, for the compromise which must be made between the conflicting requirement for the maximum power and for the maximum efficiency in MHD generators, is 0·8 [18]. An open circuit, or no net electrical current flow in the channel, occurs when the electrical field factor is 1·0.

The heat-generation parameter, η, is similar to the Brinkman number which is a criterion for the negligibility of viscous dissipation. When η is positive, heat is transferred into the system through the walls. If η is negative, heat is transferred from the fluid through the walls to the surroundings [15].

The dimensionless temperature distributions between the parallel plates at various positions in the thermal entrance region are presented in Figs. 3(a–c) and 4. In Figs. 5(a–c) and 6 the variations of dimensionless wall temperature,

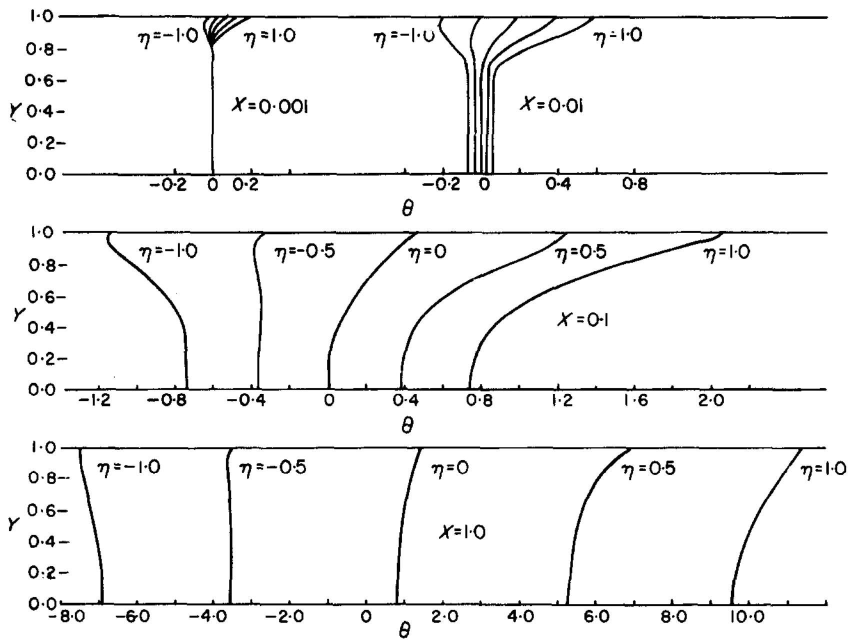

FIG. 3(a). Development of temperature profiles in the thermal entrance region $M = 4, e = 0{\cdot}5$.

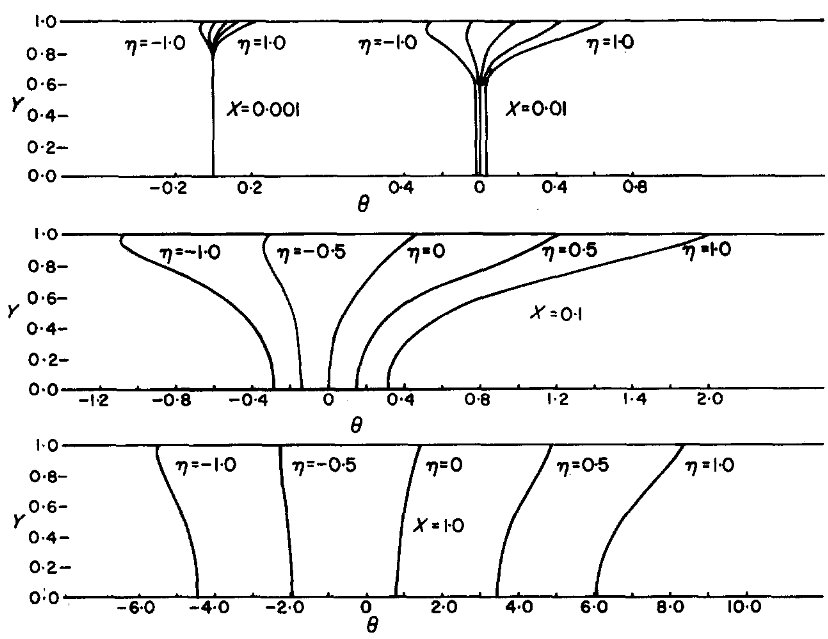

FIG. 3(b). Development of temperature profiles in the thermal entrance region $M = 4$, $e = 0{\cdot}8$.

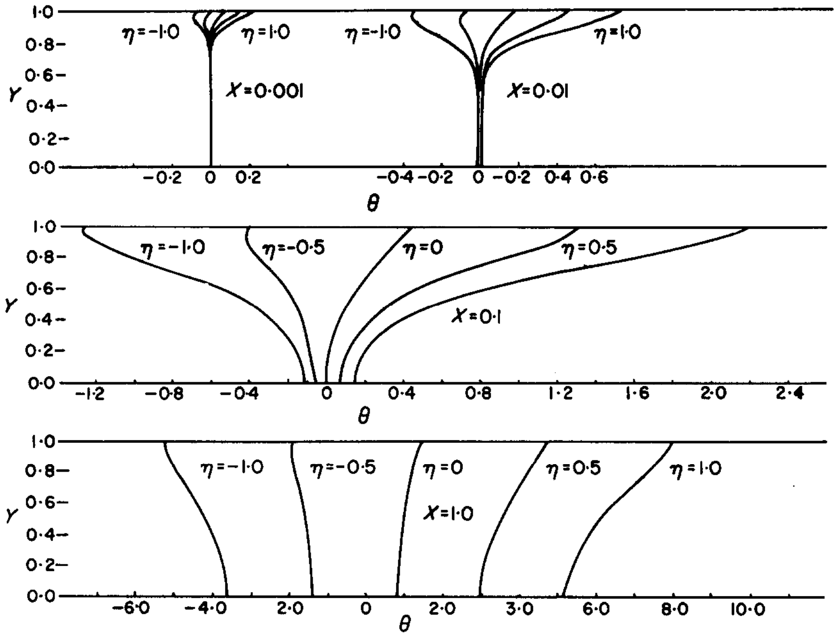

FIG. 3(c). Development of temperature profiles in the thermal entrance region $M = 4$, $e = 1{\cdot}0$.

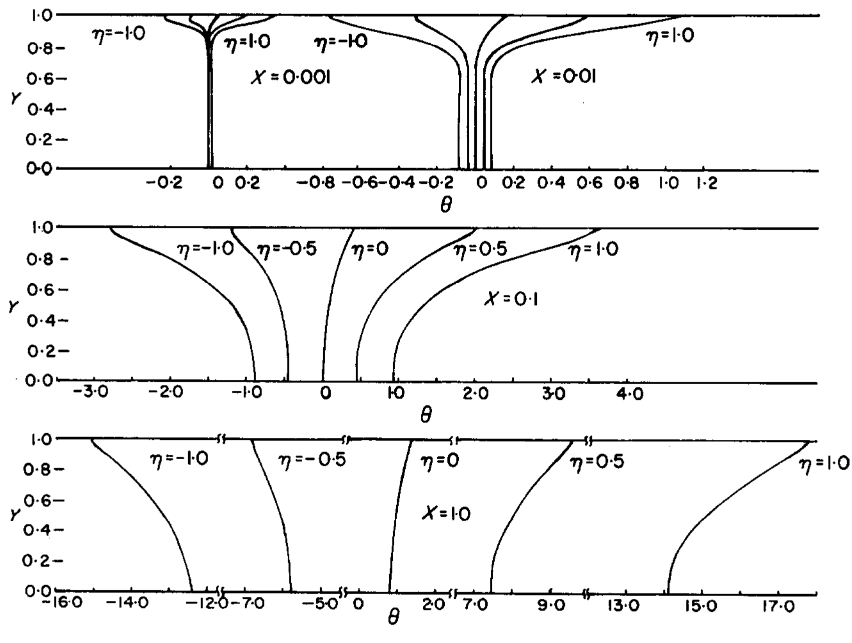

FIG. 4. Development of temperature profiles in the thermal entrance region $M = 1{\cdot}0$, $e = 0{\cdot}8$.

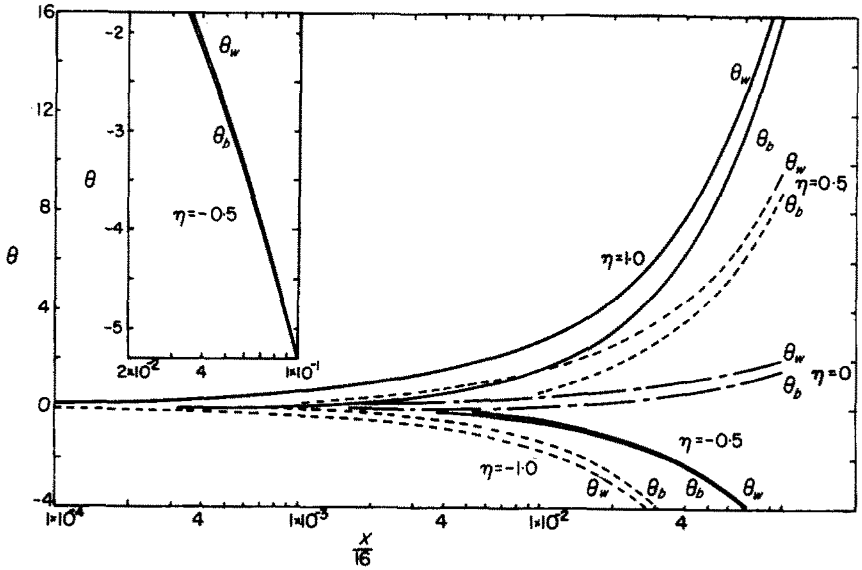

FIG. 5(a). Variation of wall and bulk temperatures, $M = 4$, $e = 0{\cdot}5$.

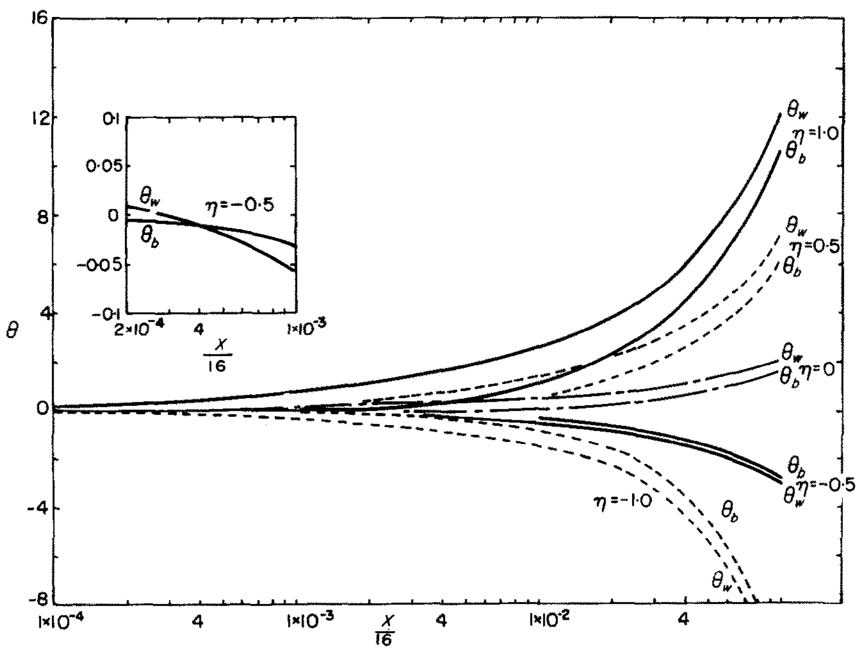

FIG. 5(b). Variation of wall and bulk temperatures, $M = 4$, $e = 0{\cdot}8$.

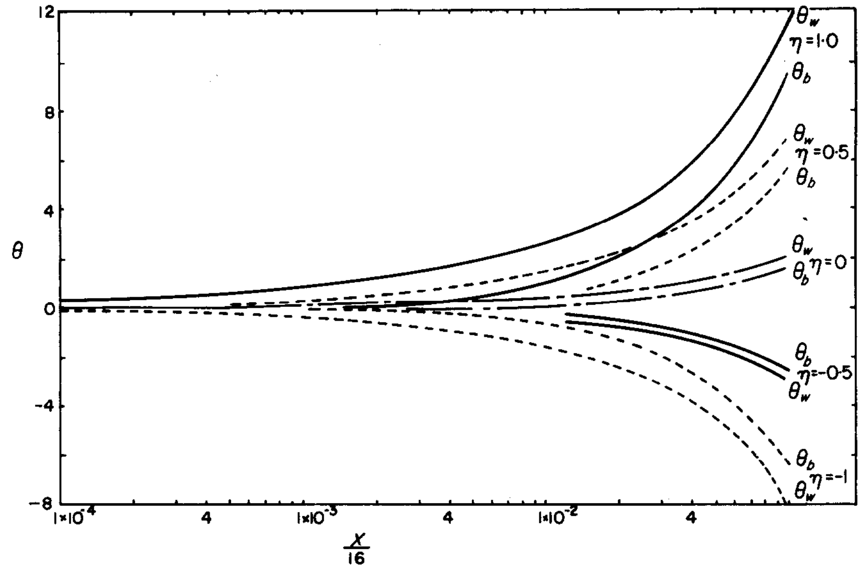

FIG. 5(c). Variations of wall and bulk temperatures, $M = 4$, $e = 1{\cdot}0$.

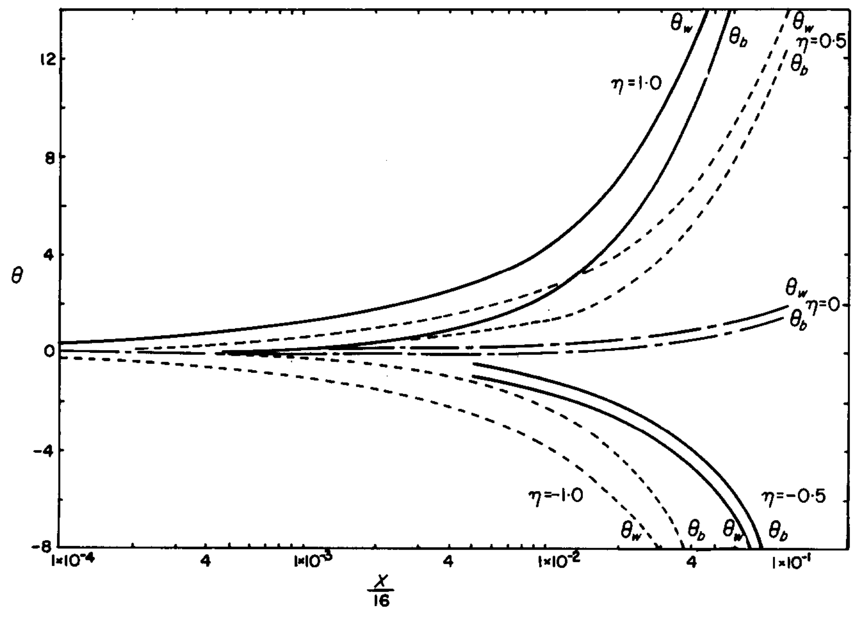

FIG. 6. Variations of wall and bulk temperatures, $M = 10$, $e = 0{\cdot}8$.

θ_w, and bulk temperature, θ_b, with dimensionless distance along the flow direction are presented. The pseudo-local Nusselt number, ψ, defined as

$$\psi = \frac{4}{\theta_{w,X} - \theta_{b,X}},$$

is plotted in Figs. 7(a–c) and 8. The quantity ψ is identical to the local Nusselt number except that it changes sign depending upon the relative magnitudes of $\theta_{w,X}$ and $\theta_{b,X}$; thus, the use of ψ reveals the behavior of the system better than the use of Nu_x. Additional numerical results are given in reference [19].

The shape of the dimensionless temperature distribution for positive values of the heat-generation parameter, η, presented in Figs. 3(a–c) and 4 is similar to those presented by Brinkman [20] for flow in a capillary with insulated walls ($q = 0$), a special case of constant heat flux at the wall. The shape of these curves, as well as those when η is less than zero, is also similar to those obtained by Novotny and Eckert [21] for free convection flow between parallel plates with uniform heat sources in the fluid. Neither of the above two references considered flow in an MHD channel.

The dimensionless temperature is uniform and equal to zero at the channel entry ($X = 0$). The temperature increases as the flow distance increases, because of heat generation by viscous dissipation and Joule heating. Since η is greater than zero when heat is added to the fluid through the wall, the combined effect of both external and internal heating is to increase the temperature of the fluid. When η is less than zero heat is transferred away from the fluid through the wall. Hence there is a competitive action between the internal heat generation and the external loss of heat. In this case, the dimensionless temperature increasing negatively is equivalent to the dimensional temperature increasing positively due to the definitions of the dimensionless temperature, θ, and the heat-generation parameter, η [15].

An increase in the electric field factor is equivalent to a decrease of electric current flow through

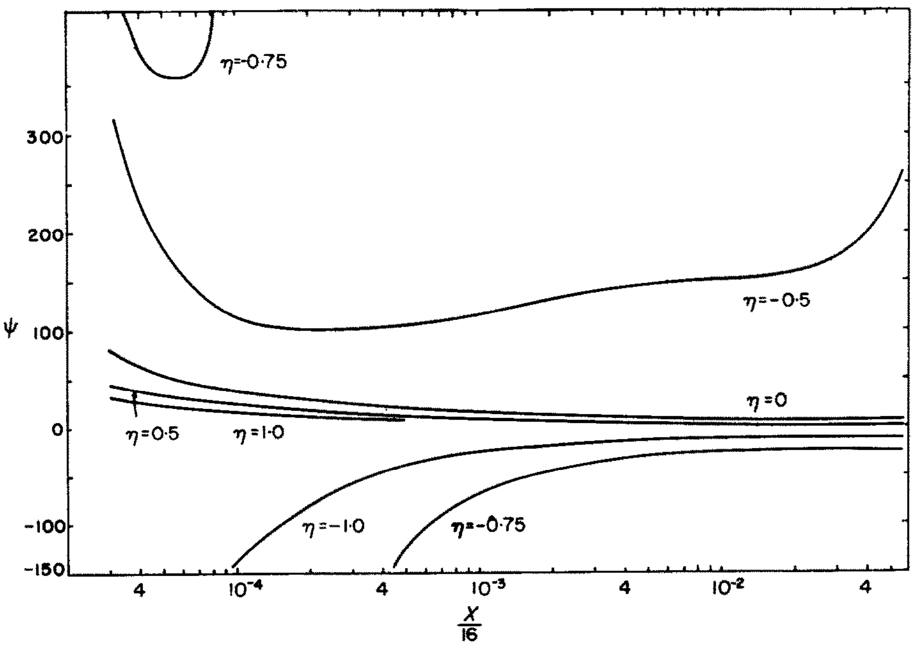

FIG. 7(a). Pseudo-local Nusselt numbers, $M = 4$, $e = 0{\cdot}5$.

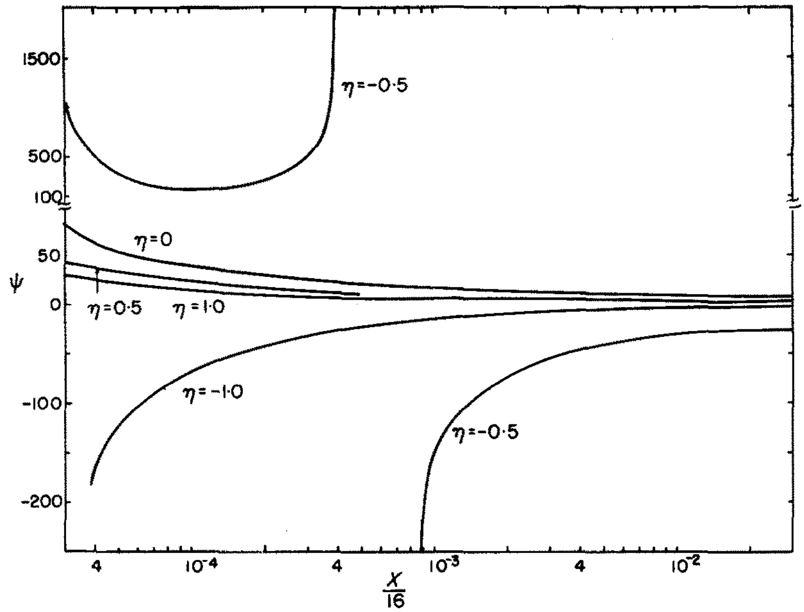

FIG. 7(b). Pseudo-local Nusselt numbers, $M = 4$, $e = 0{\cdot}8$.

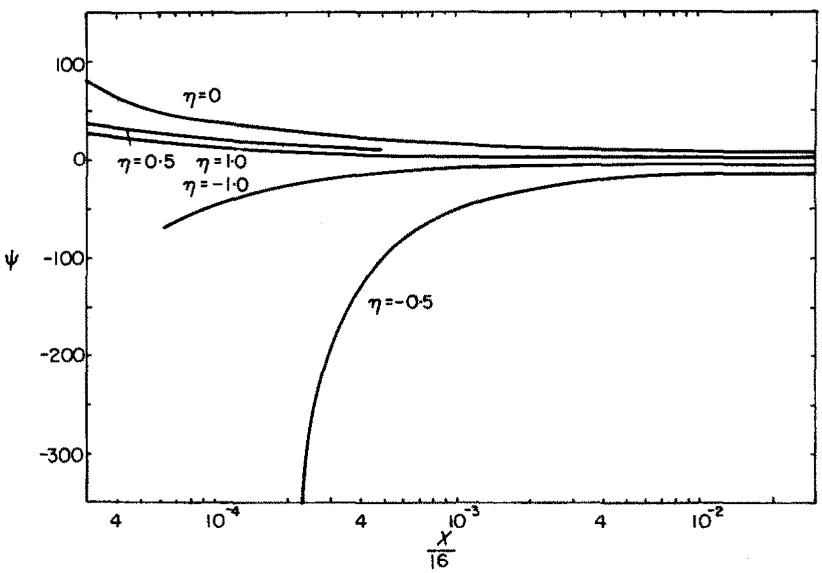

FIG. 7(c). Pseudo-local Nusselt numbers, $M = 4$, $e = 1{\cdot}0$.

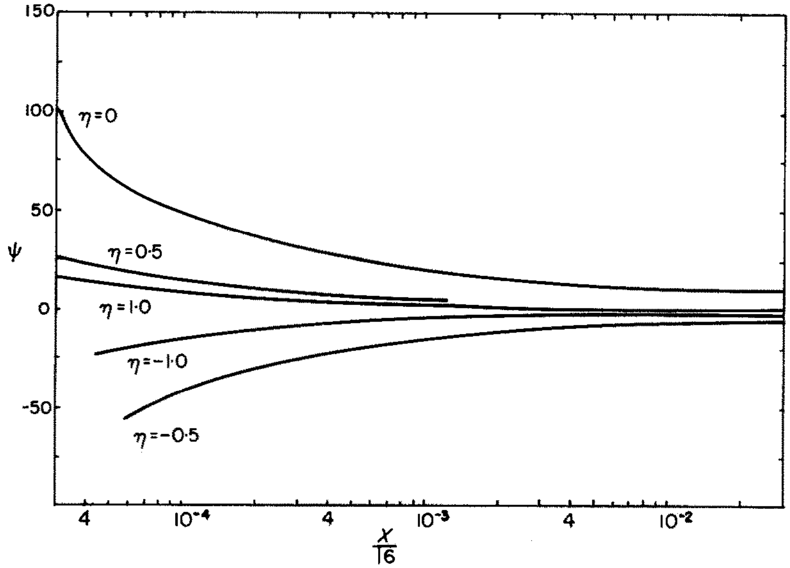

FIG. 8. Pseudo-local Nusselt numbers, $M = 1{\cdot}0$, $e = 0{\cdot}8$.

the field, and is also proportional to a decrease of Joule heating in the fluid. Comparison among Figs. 3(a), (b) and (c) for a Hartmann number of 4 shows that the rate of temperature increase is reduced by increasing e. The same trend is observed for other values of Hartmann number [19]. However, the difference between the centerline temperature and the wall temperature increases as e increases. This phenomenon is due to the increasing significance of the viscous dissipation, which is higher near the walls, as the Joule heating effect becomes smaller.

Effects of the electric field factor, e, can also be observed when a comparison is made among Figs. 5(a), (b) and (c) for Hartmann number of 4. Again, the reduction of wall and bulk temperature with increasing e can be observed, since there is a reduction in the Joule heating. The same trend can be observed for other values of Hartmann number [19]. Because of an increase in the difference between wall and bulk temperature accompanying an increase in e, there should be a decrease in the local Nusselt number, or the absolute value of the pseudo local Nusselt number, ψ, should decrease as e increases. This is shown in Figs. 7(a), (b) and (c) for Hartmann number of 4. Again the same trend can be observed for other values of Hartmann number [19].

Effects of changing the Hartmann number can readily be seen by comparing Fig. 3(b) with Fig. 4. An increase in the Hartmann number significantly increases the temperature. Similar effects can also be observed by comparing Fig. 5(b) with Fig. 6.

Effects of the heat-generation parameter, η, can be studied by examining Figs. 5(a–c) and 6. Increasing the heat-generation parameter when it is greater than zero causes an increase in the difference between the wall and bulk temperature, which in turn results in a decrease in the pseudo local Nusselt number as shown in Figs. 7(a–c) and 8. A similar trend can be seen when η is negative.

Referring to Fig. 5(a) for the case of $\eta = -0{\cdot}5$, the wall temperature, θ_w, becomes more negative than the bulk temperature, θ_b, at the position $X/16 \approx 9{\cdot}8 \times 10^{-2}$. Before this point is reached from the inlet of the duct, the temperature difference, $\Delta\theta_X = \theta_{w,X} - \theta_{b,X}$, approaches zero positively. Thus, the pseudo-local Nusselt number, ψ, should approach infinity positively.

Then at the position where the wall temperature becomes more negative than the bulk temperature, the sign of ψ is reversed and becomes negative (see Fig. 7a). A similar trend can be observed for the case in which $M = 4$, $e = 0{\cdot}8$, $\eta = -0{\cdot}5$ in Figs. 5(b) and 7(b).

Figure 9 presents a comparison of the pseudo-local Nusselt number, ψ, for various values of the Hartmann number, M. The dimensionless bulk temperature increases more rapidly than the dimensionless wall temperature as the Hartmann number increases. Therefore, for the cases in which $\eta \geqslant 0$, $\theta_{w,X} > \theta_{b,X}$, the temperature difference between the wall and bulk temperature, $\theta_{w,X} - \theta_{b,X}$ will decrease, and the pseudo-local Nusselt number, ψ, will increase [see equation (15)] as the Hartmann number increases. For the cases in which $\eta < 0$ and $\theta_{w,X} < \theta_{b,X}$, an increase in M means an increase of $\theta_{b,X} - \theta_{w,X}$ as well as a decrease of the magnitude of the pseudo-local Nusselt number, ψ.

Figure 10 shows the variation of temperature with position along the duct. The distance from the centerline is the parameter. Only one case is presented to exemplify the trend which occurs in all cases.

Figures 11(a) and (b) show the comparison of the present work with that of Michiyoshi and Matsumoto [12]. These authors assumed the viscous dissipation term to be negligible, and thus for the case of $\eta = 0$, for both Hartmann numbers of 4 and 8, the results reported by Michiyoshi and Matsumoto and those evaluated in this work should be identical. The reason that the former set of results is lower than those of the present work for small X will be explained later. For the cases in which $\eta = 0$, the results of Michiyoshi and Matsumoto differ greatly from those reported in this work. This difference is not surprising because the viscous dissipation was assumed to be negligible in the former presentation. As the Hartmann number increases the viscous term becomes less crucial and Michiyoshi and Matsumoto's results approach those reported in this work as shown in Fig. 11(b). A comparison of the results given in these figures offers an excellent opportunity to observe the effects of viscous dissipation. The comparison of results is made for the open circuit case ($e = 1{\cdot}0$) because this was the only case investigated by Michiyoshi and Matsumoto.

As stated in the introductory remarks, Perlmutter and Siegel [9] studied the same problem investigated in this work, and reported the results in the form of equations containing infinite series and, for certain special cases,

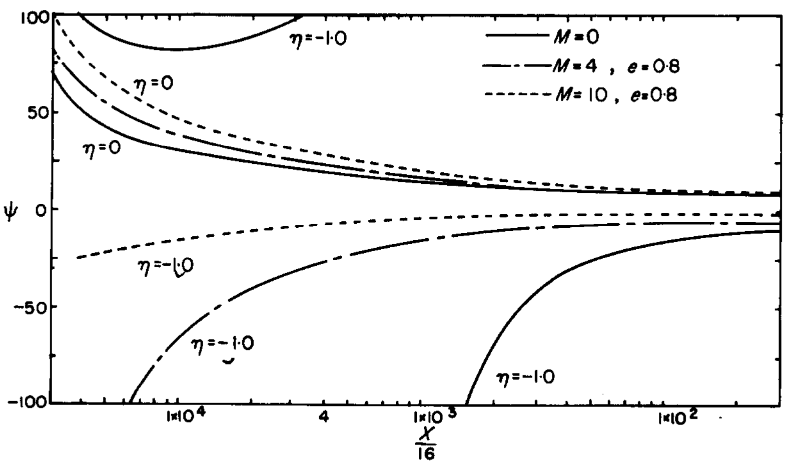

FIG. 9. Comparison of pseudo-local Nusselt numbers for various Hartmann numbers and $\eta = 0, -1{\cdot}0$.

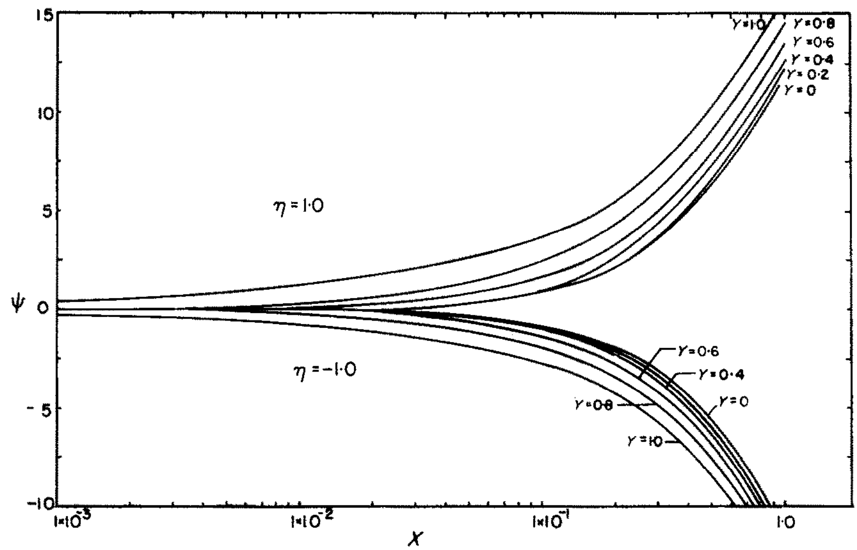

FIG. 10. Variation of temperature with position along the duct, $M = 10$, $e = 0{\cdot}8$, and $\eta = 1{\cdot}0$, $-1{\cdot}0$.

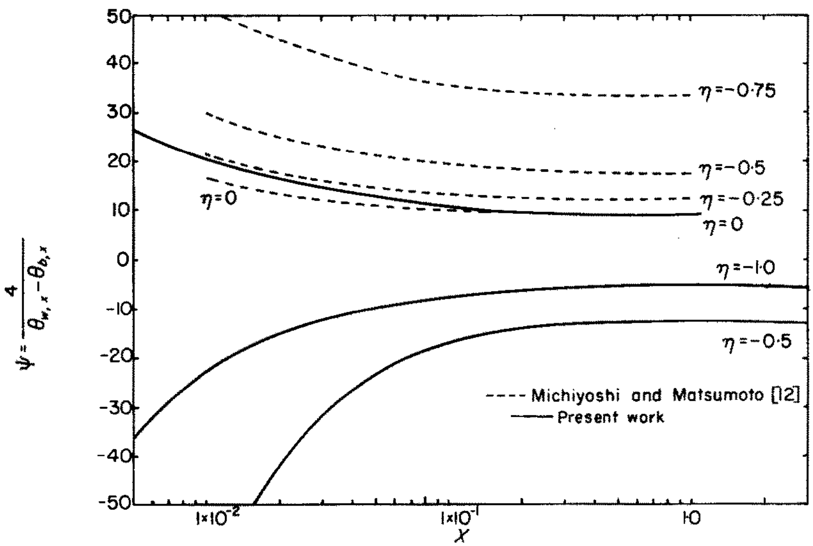

FIG. 11(a). Comparison of Nusselt number for the case $M = 4$, $e = 1{\cdot}0$.

graphical solutions are presented. Table 2 shows a comparison of the local Nusselt number for the case in which X approaches infinity and no internal heat generation in the fluid, that is for the case of $\eta = 0$, is presented for values of the Hartmann number of 4 and 10. Figure 12 compares the local Nusselt number calculated from Perlmutter and Siegel's results with the results of

Table 2. Local Nusselt number at $X \to \infty$

Hartmann number	Local Nusselt number	
	Perlmutter and Siegel [9]	Present work
4	9·1013	9·0530
10	10·2585	10·2016

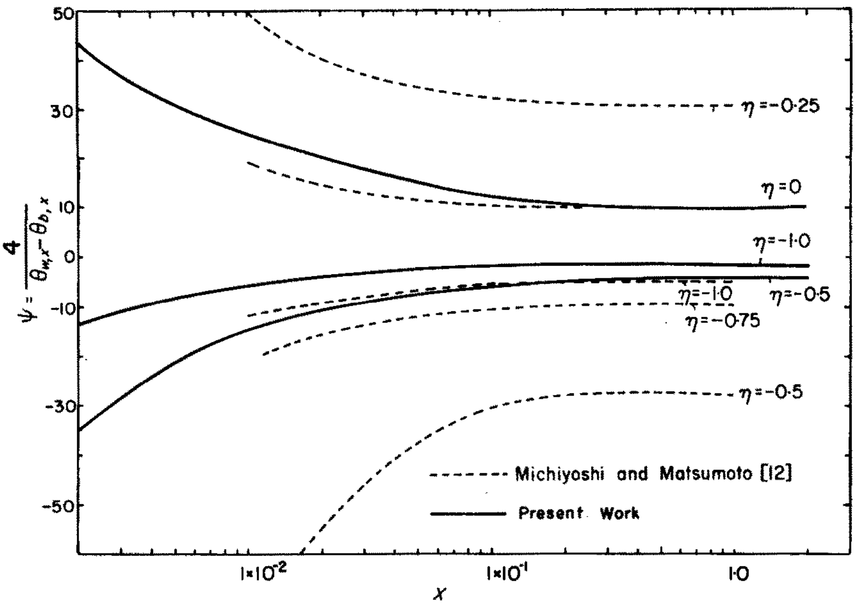

FIG. 11(b). Comparison of pseudo-local Nusselt number for the case $M = 8$, $e = 1{\cdot}0$.

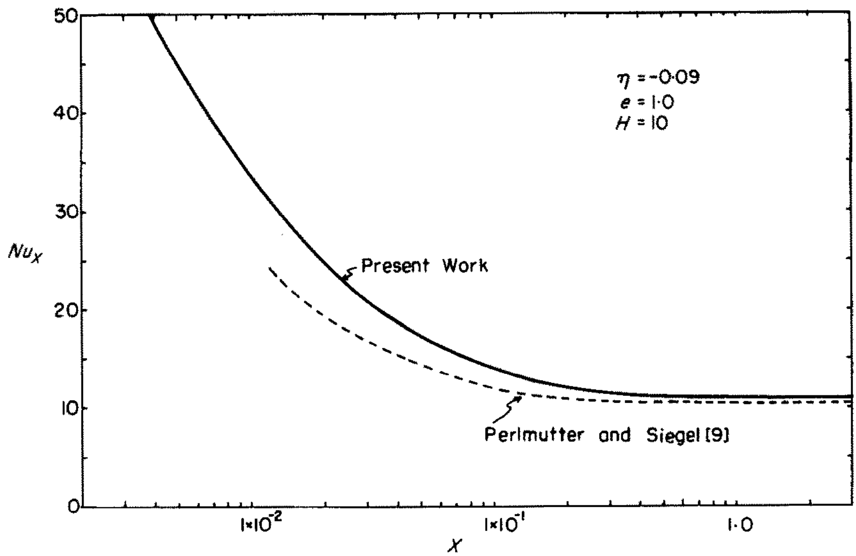

FIG. 12. Comparison of local Nusselt number for the case $M = 10$, $e = 1{\cdot}0$, $\eta = -0{\cdot}09$.

this work throughout the thermal entrance region for the case $\eta = 0{\cdot}09$, $e = 1{\cdot}0$, and $M = 10{\cdot}0$. The present work is in fair agreement with the results of Perlmutter and Siegel if X is greater than 0·3. The deviation when X is less than 0·3 perhaps is due to the error incurred when the infinite series found in Perlmutter and Siegel's solution is truncated in numerical computation. These authors reported eigenvalues for only seven terms in the infinite series; therefore, the series were probably truncated after the seventh term. A similar trend was encountered in the case of Poiseuille flow ($M = 0$, and $\eta = 0$). It was shown [15] that the results obtained by a series solution with 20 terms of eigenvalues closely agree with those obtained by the finite difference method applied in the present work, while the results obtained by the series solution with 10 terms of eigenvalues are much lower in the region of small X. The methods used in reference [9] and that in reference [12] are essentially the same. Therefore, the explanation as given above can be used to account for the discrepancy between the present results and those given in reference [9].

CONCLUSION

Forced convection heat transfer to an MHD fluid in the thermal entrance region of a flat duct is investigated in the present work. Both Joule heating and viscous dissipation are not neglected. Effects of neglecting the viscous dissipation are evaluated. Influences of the Hartmann number, heat-generation parameter, and electric field factor on the development of temperature profile and local Nusselt number are discussed.

Results are compared with those of the previous work available for some cases. It appears that the present results obtained by means of a finite difference analysis are more accurate than the previous results obtained by analytical methods.

REFERENCES

1. M. F. Romig, The influences of electric and magnetic fields on heat transfer to electrically conducting fluids, in *Advances in Heat Transfer*, edited by T. F. Irvine Jr. and J. P. Hartnett, Vol. 1, pp. 268–353. Academic Press, New York (1964).
2. R. Siegel, Effects of magnetic field on forced convection heat transfer in a parallel plate channel, *J. Appl. Mech.* **80**, 415–416 (1958).
3. R. A. Alpher, Heat transfer in magnetohydrodynamic flow between parallel plates, *Int. J. Heat Mass Transfer* **3**, 109–113 (1961).
4. J. T. Yen, Effect of wall electrical conductance on magnetohydrodynamic heat transfer in a channel, *J. Heat Transfer* **85**, 371–377 (1963).
5. W. T. Snyder, The influence of wall conductance on magnetohydrodynamic channel-flow heat transfer, *J. Heat Transfer* **86**, 552–558 (1964).
6. S. A. Regirer, On convective motion of a conducting fluid between paralled vertical plates in a magnetic field, *Soviet Phys. JETP* **37** (10) No. 1 (1960).
7. G. E. Gershuni and E. M. Zkukhovitskii, Stationary convective flow of an electrically conducting liquid between parallel plates in a magnetic field, *Soviet Phys. JETP* **34** (7), No. 3 (1958).
8. S. D. Nigam and S. M. Singh, Heat transfer by laminar flow between parallel plates under the action of a transverse magnetic field, *Q. Jl Mech. Appl. Math.* **13**, Part I, 85–96 (1960).
9. M. Perlmutter and R. Siegel, Heat transfer to an electrically conducting fluid flowing in a channel with a transverse magnetic field, NASA Technical Note D-875 (August 1961).
10. L. E. Erickson, C. S. Wang, C. L. Hwang and L. T. Fan, Heat transfer to magnetohydrodynamic flow in a flat duct, *Z. Angew. Math. Phys.* **15**, 408–418 (1964).
11. M. K. Jain and J. Srinivasan, Hydromagnetic heat transfer in the thermal entrance region of a channel with electrically conducting walls, *AIAA Jl* **2**, 1886–1892 (1964).
12. H. Michiyoshi and R. Matsumoto, Heat transfer by Hartmann flow in thermal entrance region, *Int. J. Heat Mass Transfer* **7**, 101–112 (1964).
13. J. Hartmann and F. Lazarms, *Math.-Fys. Meddr.* **6**, 15 (1937).
14. T. G. Cowling, *Magnetohydrodynamics*, Interscience, New York (1957).
15. C. L. Hwang, P. J. Knieper and L. T. Fan, Effect of viscous dissipation on heat transfer parameters for flow between parallel plates, *Z. Angew. Math. Phys.* **16**, 599–610 (1965).
16. L. Lapidus, *Digital Computation for Chemical Engineering*, pp. 254–255. McGraw-Hill, New York (1962).
17. C. L. Hwang and L. T. Fan, Finite difference analysis of forced convection heat transfer in the entrance region of a flat rectangular duct, *Appl. Scient. Res.* **A13**, 401–422 (1965).
18. W. C. Moffatt, Magnetohydrodynamic power generation—Its principles and problems, Tech. Report MIT-29-P, Project Squid, Dept. of Aerospace Engr., University of Virginia (January 1963).
19. P. J. Knieper, Heat transfer to a MHD fluid in a flat duct with constant heat flux at the walls, M.S. Thesis, Chemical Engineering Dept., Kansas State University (1965).
20. H. C. Brinkman, Heat effects in capillary flow I, *Appl. Scient. Res.* **A2**, 120–124 (1951).
21. J. L. Novotny and E. R. G. Eckert, Experimental study of laminar convection in the channel between parallel plates with uniform heat sources in the fluid, *Int. J. Heat Mass Transfer* **7**, 955–968 (1964).

Résumé—Le transport de chaleur à un fluide conducteur dans la région d'entrée thermique d'une conduite bidimensionnelle a été étudié. L'écoulement est un écoulement laminaire de Hartmann entièrement établi, et l'on suppose que le flux de chaleur est constant. Les profils de température en régime établi ainsi que le nombre de Nusselt local sont présentés graphiquement pour des valeurs du paramètre de production de chaleur égales à -1, $-0{,}5$, 0, 0,5 et 1; pour des nombres de Hartmann de 0, 4 et 10, et pour des paramètres de champ électrique de 0,5, 0,8 et 1. Les résultats présentés s'appliquent dans le cas d'un nombre de Prandtl quelconque. Certains cas sont comparés avec le travail actuel.

Zusammenfassung—Der Wärmeübergang an ein MHD-Medium in der thermischen Einlaufstrecke eines ebenen Kanals wurde untersucht. Es war eine laminare und voll ausgebildete Hartmannströmung vorhanden und der Wärmestrom an der Wand wird als konstant angesehen. Die sich ergebenden Temperaturprofile wie auch die örtliche Nusseltzahl sind graphisch wiedergegeben für einen Wärmeerzeugungsparameter von $-1{,}0$, $-0{,}5$, 0, 0,5 und 1,0; für die Hartmannzahl von 0, 4 und 10 und für den Faktor des elektrischen Feldes von 0,5, 0,8 und 1,0. Die Ergebnisse sind für Fälle beliebiger Prandtlzahl anwendbar. Für einige Fälle sind Vergleiche mit der vorangegangenen Arbeit durchgeführt.

Аннотация—Исследовался теплообмен МГД потока во входном участке плоской трубы. Течение является ламинарным и полностью развитым (поток Хартманна) и тепловой поток на стенке считается постоянным. Развивающиеся температурные профили, а также локальное число Нуссельта представлены графически для параметра образования тепла —1,0; —0,5; 0; 0,5 и 1,0; для числа Хартманна 0,4 и 10 и для напряженности электрического поля 0,5; 0,8 и 1,0. Представленные результаты можно применить к случаям с любым числом Прандтля. Проведено сравнение с результатами предыдущей работы.